Valley splitting of Si/Si$_{1-x}$Ge$_x$ heterostructures in tilted magnetic fields

K. Lai,[1] T. M. Lu,[1] W. Pan,[2] D. C. Tsui,[1] S. Lyon,[1] J. Liu,[3] Y. H. Xie,[3] M. Mühlberger,[4] and F. Schäffler[4]

[1]*Department of Electrical Engineering, Princeton University, Princeton, New Jersey 08544, USA*
[2]*Sandia National Laboratories, Albuquerque, New Mexico 87185, USA*
[3]*Department of Material Science and Engineering, UCLA, Los Angeles, California 90095, USA*
[4]*Institut für Halbleiterphysik, Universität Linz, A-4040 Linz, Austria*

We have investigated the valley splitting of two-dimensional electrons in high-quality Si/Si$_{1-x}$Ge$_x$ heterostructures under tilted magnetic fields. For all the samples in our study, the valley splitting at filling factor ν =3 (Δ_3) is significantly different before and after the coincidence angle, at which energy levels cross at the Fermi level. On both sides of the coincidence, a linear dependence of Δ_3 on the electron density was observed, while the slope of these two configurations differs by more than a factor of 2. We argue that screening of the Coulomb interaction from the low-lying filled levels, which also explains the observed spin-dependent resistivity, is responsible for the large difference of Δ_3 before and after the coincidence.

The study of the valley splitting of the two-dimensional electron gas (2DEG) confined in the (001) Si surface has been highlighted by recent research efforts on Si-based quantum computation.[1] For a Si 2DEG, only the two out-of-plane valleys are relevant since the other four in-plane valleys are lifted from the conduction band edge. To realize a functional Si quantum computer using spins as quantum bits, a large valley splitting that lifts the remaining twofold degeneracy is desirable since the existence of two degenerate states associated with the $\pm k_z$ valleys is believed to be a potential source of spin decoherence.[1] In the single-particle picture, theories[2–4] in the early period of two-dimensional (2D) physics proposed that the surface electric field in the presence of a 2D interface breaks the symmetry of these two valleys, resulting in an energy splitting proportional to the carrier density. The understanding of the valley splitting in real Si systems, however, is not trivial and requires much beyond this noninteracting band picture. In fact, a many-body effect[2,4] was speculated to account for the enhancement over the bare valley splitting under strong magnetic (B) fields, while a detailed calculation is not yet available.

Experimental research on the valley splitting, on the other hand, was conducted mainly on Si metal-oxide-semiconductor field-effect transistors (MOSFETs), in which the disorder effect is strong and direct measurement of the valley splitting proves to be difficult.[5,6] More than a decade ago, the introduction of the graded buffer scheme significantly improved the sample quality of Si/SiGe heterostructures.[7] To date, the valley splitting has been studied by various experimental techniques, including thermal activation,[8] tilted field magnetotransport,[9,10] magnetocapacitance,[11] microwave photoconductivity,[12] and magnetization.[13] However, as pointed out by Wilde *et al.* in Ref. 13, results reported by different groups are ambiguous and inconsistent with previous band calculations. The nature of this valley splitting, especially its behavior under strong B fields, stays as an unsettled problem.

Of the various methods used to study the valley splitting, tilted field magnetotransport, also known as the coincidence method,[14] is frequently utilized. In a B field tilted by an angle θ with respect to the 2D plane, the ratio of the cyclotron energy $E_c = \hbar\omega_c = \hbar eB_\perp/m^*$, where $B_\perp$ is the perpendicular field and m^* the effective mass, to the Zeeman energy $E_Z = g^*\mu_B B_{tot}$, g^* being the effective g factor and B_{tot} the total field, can be continuously tuned by adjusting $\theta = \cos^{-1}(B_\perp/B_{tot})$. In particular, the so-called coincidence happens when the energy levels from different Landau levels (LLs) are aligned at the Fermi level. In a recent experiment,[15] the intervalley energy gaps at the odd-integer quantum Hall (QH) states were studied and found to rise rapidly toward the coincidence. In this work, we show that this anomaly is not observed in the even-integer QH states, whose energy gaps close as θ approaches the coincidence. For all the samples in our study, the $\nu=3$ valley splitting before the coincidence follows a linear density dependence that extrapolates to about −0.4 K at zero density, which is probably due to level broadening. The $\nu=3$ gap after the coincidence also depends linearly on density, while the slope increases by more than a factor of 2. We argue that screening of the Coulomb interaction from the low-lying filled levels, which also explains the observed spin-dependent resistivity, is responsible for the change of the $\nu=3$ gap on different sides of the coincidence.

The specimens in our study are modulation-doped n-type Si/SiGe heterostructures grown by molecular-beam epitaxy. Important sample parameters, such as the electron density (n), mobility (μ), and width of the quantum well (W), are listed in Table I. For the samples labeled as LJxxx, relaxed Si$_{0.8}$Ge$_{0.2}$ buffers provided by Advanced Micro Devices (AMD) were used as substrates, followed by a 1 μm Si$_{0.8}$Ge$_{0.2}$ buffer layer prior to the growth of the strained Si channel. On top of the Si quantum well, a 20 nm Si$_{0.8}$Ge$_{0.2}$ spacer, a δ-doped Sb layer, a 25 nm Si$_{0.8}$Ge$_{0.2}$ cap, and a 4 nm Si cap layer are subsequently grown. The carrier density is controlled by the amount of Sb dopants. The high-mobility sample labeled as 1317 is the same specimen as that used in Ref. 15 and its density and mobility can be tuned by controlling the dose of low-temperature illumination by a light-emitting diode.

TABLE I. List of sample parameters. The density, mobility, and width of the quantum well are shown, together with the dose of illumination.

Sample	n (10^{11} cm^{-2})	μ (m^2/V s)	W (nm)	Illumination
LJ122	3.1	6.3	10	No
LJ126	2.3	9.8	10	Saturated
LJ127	2.1	8.7	10	Saturated
LJ139	1.7	12	20	Saturated
1317-I	1.4	19	15	No
1317-II	1.8	22	15	Unsaturated
1317-III	2.4	25	15	Saturated

Magnetotransport measurements were performed in the 18/20 T superconducting magnet in the National High Magnetic Field Laboratory (NHMFL) in Tallahassee, FL. Samples were placed in a rotating stage at the dilution refrigerator with a base temperature $T_{base}=20$ mK. Standard low-frequency (5–13 Hz) lock-in techniques were used to measure the diagonal resistivity ρ_{xx} and the Hall resistivity ρ_{xy}.

In Fig. 1, we show the ρ_{xx} traces as a function of the filling factor (ν) at several tilt angles for samples (a) 1317-I and (b) 1317-III. The odd-integer QH states $\nu=3,5,\dots$ are associated with energy gaps opened by the valley splitting. The three tilt angles were chosen so that from the bottom to the top traces, $1/\cos\theta=1$ (before the first coincidence), ~3.7 (between the first and second coincidences), and ~5.6 (after the second coincidence), respectively. We will return to the tilt-field data later in the discussion.

Figure 2(a) shows a schematic of the tilted-field energy diagram of a Si 2DEG. The LL (N), spin ($\uparrow$ or $\downarrow$), and valley (+ or −) indices are indicated in the plot. Since Δ_ν is shown to be independent of the parallel field,[8,15] the two valley states originating from each spin level are parallel to each

FIG. 2. (Color online) (a) Schematic of the LL fan diagram in tilted B fields. The LL (N), spin ($\uparrow$ or $\downarrow$), and valley (+ or −) indices are indicated for each level. The positions of the first and second coincidences are indicated. Measured energy gaps at (b) $\nu=4$ ($B_\perp=1.5$ T) and (c) $\nu=6$ ($B_\perp=1.0$ T) of sample 1317-I as a function of $1/\cos\theta$ or $B_{tot}/B_\perp$. The solid lines correspond to $g^*=2$.

other in the diagram. In this independent-electron picture, the levels are not affected as they cross each other, and the energy gap of individual QH states closes at certain tilt angles, or coincidence angles. Since in a Si 2DEG, Δ_ν is usually much smaller than E_Z and E_c, we adopt the conventional notation that the jth-order coincidence occurs when E_Z/E_c equals an integer j. In Figs. 2(b) and 2(c), the energy gaps, obtained by fitting $\rho_{xx}\propto\exp(-\Delta_3/2k_BT)$ in the thermal activation regime, at $\nu=4$ and 6 in sample 1317-I are shown as a function of $1/\cos\theta$ or $B_{tot}/B_\perp$. When θ is away from the coincidences, the gaps at $\nu=4$ and 6 vary linearly with respect to $1/\cos\theta$ with a slope corresponding to $g^*=2$, consistent with the independent-electron model. On the other hand, the even-integer energy gaps drop suddenly toward the coincidence angles at which the single-particle gap closes, e.g., $1/\cos\theta\sim2.5$ (first coincidence) for $\nu=4$ and $1/\cos\theta\sim4.5$ (second coincidence) for $\nu=6$, as can be seen in Figs. 2(b) and 2(c). This sudden drop of activation gap toward the degenerate points was observed in wide GaAs/AlGaAs quantum wells and explained within the framework of quantum Hall ferromagnetism.[16–18]

In contrast to the well-behaved even-integer QH states, the energy gap of the $\nu=3$ state (Δ_3) in sample LJ127 exhibits an anomalous rise toward the coincidence, as shown in the inset of Fig. 3, a phenomenon previously reported in Ref. 15. We emphasize here that this intervalley gap anomaly, observed in all the samples investigated in this study, occurs only in the coincidence region where the $\nu=3$ gap is associated with a spin-index flip rather than valley-index flip in the independent-electron picture [Fig. 2(a)]. When θ is away from the coincidence angle, the $\nu=3$ activation energy represents the valley splitting, which indeed is independent of the parallel field component. Interestingly, the valley splitting before and after the coincidence, labeled as $\Delta_3(N=0,\downarrow)$ and $\Delta_3(N=1,\uparrow)$, differs by about a factor of 3 (0.8 vs 2.1 K) for this sample.

In Fig. 3, we plot the measured $\Delta_3(N=0,\downarrow)$ and $\Delta_3(N=1,\uparrow)$ gaps for all seven samples as a function of the
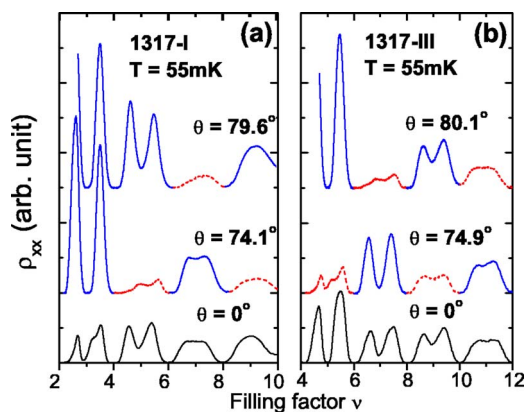

FIG. 1. (Color online) Magnetoresistivity ρ_{xx} as a function of the filling factor for samples (a) 1317-I and (b) 1317-III at selected tilt angles at $T=55$ mK. From bottom to top, the system is before the first coincidence ($\theta=0°$), between the first and second coincidences ($\theta\sim74°$), and after the second coincidence ($\theta\sim80°$). After the first coincidence, the overall amplitude of ρ_{xx} is generally higher when electrons at the Fermi level have up spins (solid curves) and lower for down spins (dashed curves).
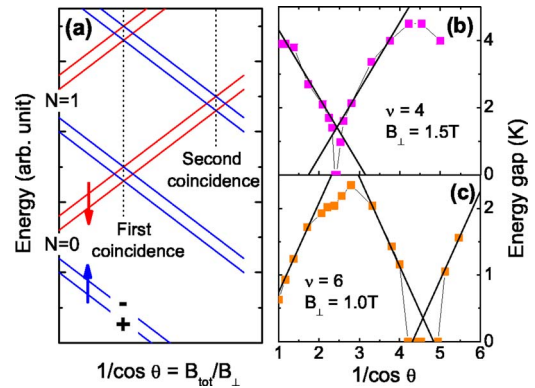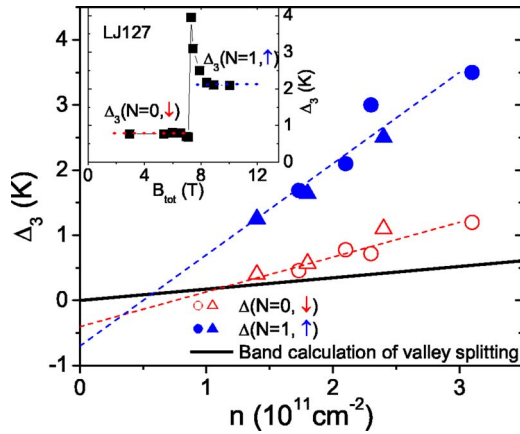
FIG. 3. (Color online) Density dependence of the valley splitting at $\nu=3$. The empty symbols (triangles for samples 1317 and circles for LJxxx) stand for $\Delta_3(N=0,\downarrow)$ and the filled symbols for $\Delta_3(N=1,\uparrow)$. Dashed lines are linear fits to the data and extrapolate to finite values at zero density. The solid line shows the band calculation of valley splitting in Ref. 2. The inset shows the Δ_3 gap of sample LJ127 as a function of B_{tot}. The coincidence occurs around $B_{\text{tot}}=7$ T.

carrier density. The band calculation of valley splitting[2–4] in a Si 2DEG based on the effective-mass approximation, showing a linear dependence Δ_v (K) $\sim 0.17n$ (10^{11} cm^{-2}) at $B=0$, is also plotted (solid line) for comparison. Despite some scattering in the data, the measured $\Delta_3(N=0,\downarrow)$ gaps essentially fall on a straight line that extrapolates to -0.4 ± 0.2 K at zero density. We note that this energy of -0.4 K is within the order of the sample-dependent disorder broadening ($\Gamma \sim \hbar/\tau = \hbar e/m^*\mu$, where τ is the transport scattering time), which lies between 0.3 and 1.1 K in our samples. The $\Delta_3(N=1,\uparrow)$ gaps of the same set of samples also fall onto a line extrapolating to -0.7 ± 0.3 K at $n=0$, again within the order of level broadening. On the other hand, the slope of the linear density dependence differs by more than a factor of 2 (0.5 vs 1.4 K per 10^{11} cm^{-2}) before and after the coincidence. And both are significantly higher than that of the band calculation at $B=0$.

Linear density dependence of the valley gaps and strong enhancement over the bare valley splitting were recently reported in both Si MOSFET (Ref. 11) and wide-well AlAs systems[19] and attributed to the effect of exchange interaction.[11] The large difference between the $\Delta_3(N=0,\downarrow)$ and $\Delta_3(N=1,\uparrow)$ gaps, however, is not observed in these systems. Since the LL indices are different for these two gaps, it is natural to first consider the additional exchange-correlation contribution (E_{xc}) to the electronic energy.[20,21] In this Hartree-Fock picture, the difference between energy gaps on either side of the coincidence is simply the difference between the exchange-correlation energies of the $N=0$ and LLs, irrespective of valley splitting. However, such an analysis contradicts our experimental results in that it predicts a smaller $\Delta_3(N=1,\uparrow)$ than $\Delta_3(N=0,\downarrow)$, since E_{xc} of the top filled $N=1$ LL is smaller than that of the $N=0$ LL. Alternatively, we propose a different scenario. In Fig. 4, the two configurations of $\nu=3$ are shown for comparison. Since the electron-electron (e-e) interaction energy $E_{e-e} \sim e^2/4\pi\epsilon l_B$
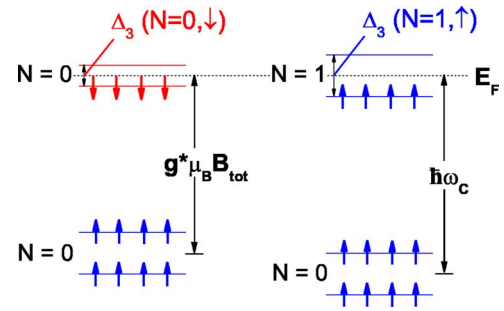

FIG. 4. (Color online) Level diagram at $\nu=3$ before (left) and after (right) the coincidence. E_F resides in the gap between the lowest empty levels and the top filled levels. The level occupation, as well as the spin orientation, is indicated in the plot. Before the coincidence, the low-lying ($N=0,\uparrow,\pm$) electrons, separated by $E_Z=g^*\mu_B B_{\text{tot}}$ from the Fermi level, strongly screen the Coulomb interaction for electrons near E_F, resulting in a less enhanced $\Delta_3(N=0,\downarrow)$ over the bare valley splitting. The same screening, on the other hand, is less effective from the like-spin charges in a different LL, giving a large $\Delta_3(N=1,\uparrow)$.

$[l_B=(\hbar/eB_\perp)^{-1/2}$ is the magnetic length] is comparable to the LL or spin splitting for the relevant perpendicular B fields in this work, we explicitly include the lower two filled levels ($N=0,\uparrow,\pm$) in the analysis. Before the coincidence, electrons in these two low-lying levels have the same LL but opposite spin indices compared to the ones near the Fermi level (E_F). Since the Pauli exclusion principle does not prevent the opposite spins from approaching each other, these low-lying electrons can come close to the electrons at E_F and strongly screen the Coulomb interaction. The enhancement of the $\nu=3$ gap due to the electron-electron interaction is thus much reduced and the gap is close to the bare value at this LL. On the other side of the coincidence, however, such screening is much less effective. First, the electrons near E_F are from the $N=1$ LL and their wave function is different from that of the $N=0$ levels. The off-diagonal matrix element of this Coulomb energy between the two different LLs should be considerably smaller than that from the same LL. Second, even in the presence of the LL mixing effect, the exclusion principle limits the screening between the same up-spin levels. As a result, the $\Delta_3(N=1,\uparrow)$ gap is greatly enhanced over the bare valley splitting. We nevertheless emphasize here that in the last few LLs, the shape of the wave function is completely different from the plane wave at $B=0$. So even the bare valley splitting here could be different from the results obtained by Ohkawa and Uemura,[2] who only consider high LLs by using a simple average over the in-plane k vector.

Finally, we note that the spin-dependent resistivity, first reported by Vakili et al.[22] in a narrow-well AlAs system and successfully explained by screening from the filled LLs, is also observed in our samples. In Fig. 1, after the first coincidence, the overall ρ_{xx} amplitude is lower (dashed curves) when spins at the Fermi level orient opposite to the majority up spins in the system and higher when the two are aligned (solid curves). Due to the exclusion principle, like-spin electrons cannot approach each other to effectively screen the disorder potential, resulting in a higher ρ_{xx} compared to the

opposite case. Interestingly, the same alternating pattern is also observed in the strengths of the odd-integer valley states.

In summary, we have carried out a tilted-field study of $Si/Si_{1-x}Ge_x$ heterostructures. The energy gaps at the even-integer QH states follow qualitatively the independent-electron picture, while the gaps at the odd-integer states show rapid rise toward the coincidence angles. For all the samples we studied, the $\nu=3$ valley splitting on both sides of the coincidence shows linear density dependence. The difference of the $\Delta_3(N=0,\downarrow)$ and $\Delta_3(N=1,\uparrow)$ gaps, as well as the observed spin-dependent resistivity, can be qualitatively explained by screening of the Coulomb interaction from the low-lying filled levels.

[1] M. Xiao, I. Martin, E. Yablonovitch, and H. W. Jiang, Nature (London) **430**, 435 (2004), and references therein.

[2] F. J. Ohkawa and Y. Uemura, J. Phys. Soc. Jpn. **43**, 917 (1977).

[3] L. J. Sham and M. Nakayama, Phys. Rev. B **20**, 734 (1979).

[4] T. Ando, A. B. Fowler, and F. Stern, Rev. Mod. Phys. **54**, 437 (1982).

[5] R. J. Nicholas, K. von Klitzing, and T. Englert, Solid State Commun. **34**, 51 (1980).

[6] V. M. Pudalov, S. G. Semenchinski, and V. S. Edel'man, JETP Lett. **41**, 325 (1985).

[7] F. Schäffler, Semicond. Sci. Technol. **12**, 1515 (1997), and references therein.

[8] P. Weitz, R. J. Haug, K. von Klitzing, and F. Schäffler, Surf. Sci. **361/362**, 542 (1996).

[9] S. J. Koester, K. Ismail, and J. O. Chu, Semicond. Sci. Technol. **12**, 384 (1997).

[10] H. W. Schumacher, A. Nauen, U. Zeitler, R. J. Haug, P. Weitz, A. G. M. Jansen, and F. Schäffler, Physica B **256-258**, 260 (1998).

[11] V. S. Khrapai, A. A. Shashkin, and V. T. Dolgopolov, Phys. Rev. B **67**, 113305 (2003).

[12] S. Goswami, M. Friesen, J. L. Truitt, C. Tahan, L. J. Klein, J. O. Chu, P. M. Mooney, D. W. van der Weide, S. N. Coppersmith, R. Joynt, and M. A. Eriksson, cond-mat/0408389 (unpublished).

[13] M. A. Wilde, M. Rhode, C. Heyn, D. Heitmann, D. Grundler, U. Zeitler, F. Schäffler, and R. J. Haug, Phys. Rev. B **72**, 165429 (2005).

[14] F. F. Fang and P. J. Stiles, Phys. Rev. **174**, 823 (1968).

[15] K. Lai, W. Pan, D. C. Tsui, S. Lyon, M. Mühlberger, and F. Schäffler, Phys. Rev. Lett. **96**, 076805 (2006).

[16] K. Muraki, T. Saku, and Y. Hirayama, Phys. Rev. Lett. **87**, 196801 (2001).

[17] V. Pellegrini, A. Pinczuk, B. S. Dennis, A. S. Plaut, L. N. Pfeiffer, and K. W. West, Science **281**, 799 (1998).

[18] V. S. Khrapai, E. V. Deviatov, A. A. Shashkin, V. T. Dolgopolov, F. Hastreiter, A. Wixforth, K. L. Campman, and A. C. Gossard, Phys. Rev. Lett. **84**, 725 (2000).

[19] Y. P. Shkolnikov, E. P. De Poortere, E. Tutuc, and M. Shayegan, Phys. Rev. Lett. **89**, 226805 (2002).

[20] M. L. Glasser and Norman J. Morgenstern Horing, Phys. Rev. B **31**, 4603 (1985).

[21] A. H. MacDonald and D. S. Ritchie, Phys. Rev. B **33**, 8336 (1986).

[22] K. Vakili, Y. P. Shkolnikov, E. Tutuc, N. C. Bishop, E. P. De Poortere, and M. Shayegan, Phys. Rev. Lett. **94**, 176402 (2005).